Efficient Numerical Simulation of the Time Dependence of Electronic Energy Transfer in Polymers. 1. Short-Range Transfer and Trapping

Jeffrey D. Byers, Mark S. Friedrichs, Richard A. Friesner, and S. E. Webber*

Department of Chemistry, The University of Texas, Austin, Texas 78712.
Received February 18, 1988; Revised Manuscript Received May 27, 1988

ABSTRACT: The Lanczos method has recently been applied to the problem of transport on disordered lattices. In this method the master equation is solved directly without resort to approximate analytical solutions or physically unrealistic limiting cases. We apply this method to electronic energy transport (EET) on a polymer coil embedded in a cubic lattice as a function of coil expansion in order to assess the importance of cross-chain EET. A simple model system is examined in which deep traps are placed randomly or on chain ends and EET occurs only between adjacent points on the cubic lattice. The highly nonexponential decay curves are analyzed as follows: (1) weighted distribution of exponentials (eigenvalue distribution), (2) moment analysis, (3) least-squares fit to a "generalized stretched exponential" ($\exp(-At^{d/2} + Bt^{d} - Ct^{3d/2})$) where d is nonintegral, and (4) a time-dependent fractal dimensionality ($\exp(A(t)t^{\alpha(t)})$). The point of these analyses is to guide the interpretation of experimental data in physical systems in which the degree of cross-chain EET is unknown.

Introduction

In recent years there has been a great deal of activity in the general area of polymer photophysics. One aspect of this subject is the transfer of excitation along a chain by what is presumed to be a random walk between pendant chromophores. This excitation can continue to be transferred until (1) spontaneous emission occurs (singlet or triplet), (2) two excitations encounter each other leading to excited state annihilation, (3) the excitation self-traps (usually leading to excimer fluorescence), or (4) the excitation encounters a trapping species, in which case sensitized trap fluorescence may be observed. The trap may also be a pair of chromophores appropriately oriented for facile excimer formation (the so-called "excimer forming site"). There is no a priori way to distinguish excimer formation by rotation of a ground-state and excited-state chromophore to form an excimer from energy migration to an excimer-forming site.

It is tempting to think of the motion of the excitation to be essentially one dimensional with random placement of traps; a rather detailed analysis of excimer fluorescence based on this type of model has been presented by Frank and co-workers.[1] Certainly one expects the density of excimer-forming sites to be dependent on the polymer structure and the type of chromophore, but the energy-transfer processes themselves also will depend on these properties through the following: (1) the distribution of chromophore–chromophore separations, which in turn will depend on the polymer tacticity, mode of chromophore attachment, and molecular weight; (2) the distribution of chromophore–chromophore orientations, since in general the rate of energy transfer between two chromophores is anisotropic; (3) the distance over which energy transfer occurs, which will depend on the properties of the chromophores. Items 1 and 2 will also depend strongly on the solvent and temperature in general. Thus one would expect polymer systems to behave as highly disordered one-dimensional systems in the simplest cases. However, the distance over which energy is transferred can be sufficiently large that nonadjacent chromophores are involved. Thus cross-chain energy transfer can occur and the system is no longer strictly one dimensional.

As is obvious from the above qualitative discussion, the kinetics and structure–property relationships of excited-state processes in polymers are very complex. Additionally there are a very large number of ways in which a given chromophore can be incorporated onto a polymer coil. This article will concern itself with our recent efforts to model excited-state kinetics for a simple polymer model which contains the essential features of realistic physical systems. A rigid polymer coil is embedded in a cubic lattice and energy transfer is allowed between adjacent sites (whether bonded or nonbonded) on this lattice; this transfer law corresponds most closely to triplet excitation transport, where the intermolecular interactions are very weak. The traps interspersed along the coil are taken to be infinitely deep and to have a single lattice constant as their radius of capture. The formalism used to generate polymer configurations (ranging from extended to collapsed conformations) is a standard excluded-volume model[2,3] with a single parameter defining the strength of the nonbonded nearest-neighbor interactions.

The general objectives of this work are (1) to carry out a set of numerical simulations of the excitation dynamics for polymer ensembles of varying length and average conformation which are quantitatively accurate over the entire time regime of interest; (2) to extract from these results a qualitative understanding of the dependence of experimentally observable fluorescence decays on polymer conformation, trap density and placement, and other parameters; and (3) to propose and evaluate approaches for determining these quantities directly from experimental data. The results reported below obviously represent only a beginning of these tasks; a large number of modifications of the basic model are possible, and many quite different models corresponding to more complex physical systems can be constructed. Some of these will require significant alterations in our computational methods (e.g., incorporations of polymer motion), while others (Förster energy transfer law, larger trap radius, study of polymer melts) will not.

To accomplish these objectives, we have developed a novel methodology for computing the survival probability of an excitation obeying a Pauli master equation. In contrast to approximate methods (e.g., cumulant expansions) which have been used previously, our results are reliable to machine accuracy for all times, polymer geometries, and trap densities. Furthermore, large computation time reductions are routinely achieved as compared to straightforward diagonalization of the transfer matrix, the usual means of obtaining accurate numerical results; for a single polymer of length 1000, a 3 order of magnitude advantage (0.1 CPU s versus 100 CPU s) is observed on a Cray X-MP supercomputer. This combination of general

0024-9297/88/2221-3402$01.50/0

applicability and efficiency allows us to analyze any polymer model that we are capable of generating (indeed, the computation time needed to do this is typically at least as large as that required to compute the dynamics) and to focus on interpretations of the results without fear of biasing due to inaccurate data. We have chosen to explore a variety of approaches to analysis of the decay functions, including examination of moments, eigenvalue distributions, and fitting procedures based on concepts of fractal geometries. While a definitive assessment of the merits of each technique awaits further simulations and investigation of actual experimental data, some conclusions can be drawn about the utility of these procedures. In particular, it is shown that care must be taken to avoid contamination by finite size effects in a fractal analysis. Our goal is to provide accurate numerical experiments based on a model frequently invoked in polymer photophysics: a nearly 1-D finite lattice with randomly placed disruptive (i.e., irreversible) traps. We hope to find the "signature" of this model in the time-dependence of the donor excited state that will permit the experimentalist to know if a physical system under investigation can be thought of in this way. In future work this model will be elaborated to permit explicit consideration of (1) sequence distribution in copolymers, (2) tacticity, and (3) correlation of EET rates that might arise from nearest-neighbor packing requirements.

Methods

A. Numerical Solution of the Time-Dependent Equations. The ensembled averaged excitation survival probability, $S(t)$, is determined in two major steps. In the first the polymer coils and their associated weights are generated so that the resulting ensemble is consistent with a specified temperature and interaction energy between adjacent, but unbonded, segments (contact bonds). In the second step the survival probability for each of the resulting configurations is calculated, and the ensemble average of this quantity is constructed. In this section, we describe the methods used to solve the master equation for a given configuration; the generation of the static coil structure is addressed in the next subsection.

$S(t)$ may be expressed in terms of a diagonal matrix element of the Pauli master equation's Green's function. The salient features involved in numerically determining the matrix element via the Lanczos algorithm and recursive residue generation method (RRGM) are outlined in the following. A more detailed description of the numerical considerations involved in implementing the procedure is provided elsewhere,[4] along with a brief discussion of the relative merits of this approach vis-à-vis alternative methods.

Given a polymer comprised of M chromophores (excluding trap sites), the diffusion of the excitation on the coil is modeled by the Pauli master equation

$$\frac{dp_i(t)}{dt} = \sum_{j=1}^{M} w_{ij}p_j(t) - (w_{ji} + u_i)p_i(t) \quad (1)$$

Here $p_i(t)$ is the probability chromophore i is occupied by the excitation at time t, w_{ij} is the excitation transfer rate from chromophore j to chromophore i, and u_i is the total transfer rate of the excitation from chromophore i to all traps present on the polymer. Equation 1 can be written in matrix form as

$$d\mathbf{P}(t)/dt = \mathbf{W}\mathbf{P}(t) \quad (2)$$

where the ith element of $\mathbf{P}(t)$ is $p_i(t)$ and the transfer rate matrix $\mathbf{W}$ is the $M \times M$ array with $[W]_{ij} = (1 - \delta_{ij})w_{ij} - \delta_{ij}(u_i + \sum_k w_{ik})$ [δ_{ij} is the Kronecker δ]. The trap sites are excluded from eq 1 and 2 since it is assumed that the excitation is instantaneously quenched at its first encounter of a trap; hence the back-transfer rates from the traps to the chromophores are zero so that the trapping rates only appear in the diagonal entries of $\mathbf{W}$. For the set of calculations presented here, only nearest-neighbor transfer is considered, and we have set the time unit so that the nonzero transfer rates are one ($w_{ij} = 1$ if chromophores i and j are adjacent and $w_{ij} = 0$ otherwise). Likewise, u_i is simply the number of traps adjacent to the chromophore i. In later work more realistic distant and orientation-dependent transfer rates (e.g., Forster and Dexter transfer rates) will be applied.

The formal solution of eq 2 is

$$\mathbf{P}(t) = \exp(\mathbf{W}t)\mathbf{P}(t=0) = \mathbf{G}(t)\mathbf{P}(t=0) \quad (3)$$

where $\mathbf{P}(t=0)$ is the excitation's initial occupation distribution on the polymer. The matrix element of Green's function in the site representation $G_{ij} = \langle i|\mathbf{G}(t)|j\rangle$ is the conditional probability that chromophore i is occupied by the excitation at time t given chromophore j was initially occupied. Consequently, for an arbitrary initial occupation distribution, the probability that chromophore i is occupied at time t is

$$p_i(t) = \sum_{j=1}^{M} G_{ij}(t)p_j(0) \quad (4)$$

and the survival probability of the excitation is

$$S(t) = \sum_{i=1}^{M}\sum_{j=1}^{M} G_{ij}(t)p_j(0) \quad (5)$$

If each chromophore is equally likely to be occupied at $t = 0$, the $p_j(0) = (1/M)$, and hence

$$S(t) = \frac{1}{M}\sum_{i=1}^{M}\sum_{j=1}^{M} G_{ij}(t) = \frac{1}{M}\langle f|\mathbf{G}(t)|f\rangle = \frac{1}{M}G_{ff}(t) \quad (6)$$

where $|f\rangle$ is the vector of dimension M with each entry equal to one.

The diagonal Green's function matrix element $G_{ff}(t)$ can be expressed in terms of $\mathbf{W}$'s eigenvalues, $\{\lambda_i\}$, and eigenvectors, $\{|\lambda_i\rangle\}$. Inserting the complete set of $\mathbf{W}$'s eigenstates into eq 6 yields

$$G_{ff}(t) = \langle f|\exp(\mathbf{W}t)|f\rangle = \sum_{j=1}^{M}|\langle f|\lambda_j\rangle|^2 e^{\lambda_j t} = \sum_{j=1}^{M} R_{ff}^{(j)}e^{\lambda_j t} \quad (7)$$

where $R_{ff}^{(j)}$ is referred to as the residue of λ_j.

The eigenvalues and residues of eigenstates which are strongly coupled to $|f\rangle$ (strong in the sense of a relatively large residue) are calculated by utilizing the Lanczos algorithm and RRGM. Both these sets of quantities are found by first using the Lanczos procedure to generate a symmetric, tridiagonal matrix $\mathbf{T}$ which is related to $\mathbf{W}$ by a similarity transformation.[5] The eigenvalues of $\mathbf{T}$ are then determined by using a vectorized version of the bisection algorithm.[6] In exact arithmetic the eigenvalues of $\mathbf{W}$ and $\mathbf{T}$ are identical. However, the Lanczos procedure is numerically unstable, and as a result the spectra of the two matrices are not completely isomorphic. The origin of this breakdown in the structure of $\mathbf{T}$'s spectrum has been recently illuminated, and the problems associated with this instability are easily circumvented.[7-9]

The projections $|\langle f|\lambda\rangle|^2$ are determined via the residue theorem,[10] which forms the basis of the RRGM. According to this approach the residues can be calculated from the spectra of $\mathbf{T}$ and $\mathbf{T}'$ (the matrix obtained by deleting the first row and column of $\mathbf{T}$) by choosing the initial Lanczos

vector to be $|f\rangle$. Thus in lieu of explicitly calculating the eigenvectors of $\mathbf{W}$—an inefficient approach when, as here, only one or a few of $\mathbf{G}(t)$'s matrix elements are required—the residues are simply found by diagonalizing two tridiagonal matrices. Once the eigenvalues and residues have been determined, the survival probability for the given polymer configuration is assembled by using eq 7, and the result with the appropriate weight is included in the ensemble average (see eq 10 in the following).

B. Simulation of Coils. The method employed to generate the polymer configurations was a modified Rosenbluth and Rosenbluth[2] Monte Carlo technique, similar to that used by McCrackin et al.[3] For the simple Monte Carlo technique each step of the polymer configuration is generated a priori one step at a time. The potential energy of each configuration is calculated by using some model and the average over an ensemble of configurations of any property is given by

$$\langle F \rangle = \sum_{i=1}^{m} F_i e^{-U_i/kT} / \sum_{i=1}^{m} e^{-U_i/kT} \tag{8}$$

where U_i is the energy of the ith configuration and m is the total number of configurations generated. However, to achieve any reasonable degree of accuracy requires a very large number of configurations. Importance sampling has been used to reduce the size of the ensemble. A brief description of this method follows: At each step all possible sites are weighted by the energy change that would result from a particular step. Then one step is chosen at random by using the weighted probabilities ρ_j. This process is repeated until a polymer of size N is created. The probability of generating any given configuration is then

$$\pi_i = \prod_{j=1}^{N} \rho_j = \prod_{j=1}^{N} \frac{e^{-u_j/kT}}{\sum_{k=1}^{n} e^{-u_k/kT}} \tag{9}$$

where u_j is the energy associated with the jth step actually taken and the sum over k includes all possible moves for the jth step. The average over the ensemble for any observable is

$$\langle F \rangle = \frac{\sum_{i=1}^{m} F_i \pi_i^{-1} e^{-U_i/kT}}{\sum_{i=1}^{m} \pi_i^{-1} e^{-U_i/kT}} = \frac{\sum_{i=1}^{m} F_i w_i}{\sum_{i=1}^{m} w_i} \tag{10}$$

For the cases that this procedure works very well (see below), the weights used in the equation for the average over the ensemble are fairly constant, and a small number of samples is needed. However, for some cases, the procedure is not very efficient; the weights may vary over 4 orders of magnitude and only a few samples contribute to the ensemble average. A large number of samples must then be generated to ensure a good representation of the ensemble. Some of this added time can be saved by calculating the quantities of interest only for those samples that have an appreciable weighting.

In generating our configurations we confined the polymer to a 3-D cubic lattice and used a square-well potential to calculate the energy of the configurations. The square-well potential depends only on the distance between two nonbonded chromophore sites.

$$u(r) = \begin{bmatrix} \infty, r = 0 \\ -\epsilon, r = a \\ 0, r > a \end{bmatrix} \qquad a = \text{lattice spacing} \tag{11}$$

This model allows for self-avoidance in solutions of various strengths. Introducing the parameter $\phi = -\epsilon/kT$, the average over the ensemble becomes

$$\langle F \rangle = \frac{\sum_{i=1}^{m} F_i \pi_i^{-1} e^{c_i \phi}}{\sum_{i=1}^{m} \pi_i^{-1} e^{c_i \phi}} \tag{12}$$

where c_i is the number of contacts between nonbonded chromophores (those sites that are separated by only one lattice spacing). Much previous work has been focused on two specific cases for this model, $\phi = 0$ (the hard-sphere model) and $\phi = 0.275$ (the Flory Θ-point). We chose to consider cases ranging from a "very good" solvent ($\phi = -0.5$, e.g., contact repulsion) to a very poor one ($\phi = 0.5$), including both the hard-sphere ($\phi = 0$) and Θ-point case ($\phi \approx 0.275$). Also included in the study was the infinitely repulsive case ($\phi = -\infty$) in which no contacts are required. Since this case is strictly one dimensional it is not necessary to obtain an ensemble of chains. The length of the polymer was varied from 50 to 800 chromophore sites, but the chain statistics are poor for the latter case such that we report the results up to length 400 in most cases.

Two quantities commonly calculated in polymer simulations are the mean-square radius of gyration and the mean-square end-to-end distance. We calculated these quantities both for validation of our program and for correlation to the kinetic decay (see later section). One of the checks employed on our technique requires the plotting of these two quantities against the length of the polymer for the various solvent strengths. It has been shown that the relationship $\langle R^2 \rangle \propto N^a$ should be obeyed where $a = 1.2$ for the hard-sphere model and $a = 1.0$ at the θ-point.[3] We find the values 1.16 (±0.03) and 1.0 (±0.01), respectively, for these two quantities (uncertainty based on multiple ensembles and a weighted-least-squares fit). As is well-known, the statistics of an ensemble of self-avoiding chains become more unreliable as the length of the chains increases and as ϕ becomes larger than the Θ-point value. This is seen to be the case in the standard deviation of the quantities tabulated in Table I. Despite the larger scatter in all quantities calculated for $N \geq 400$ and $\phi > 0.275$ all results in this range seem to extrapolate smoothly from the statistically more favored N, ϕ range and we believe they are reasonably accurate.

Once a configuration is obtained, some of the chromophore sites are designated as traps. Then a transfer matrix $\mathbf{W}$ is constructed (see previous section) and the decay as a function of time for the given polymer configuration is calculated. This decay is averaged over the ensemble by using eq 10. The transfer matrix is constructed such that the i-jth coefficient is given by the rate of transfer from chromophore i to chromophore j and the diagonal element i-i is given by minus the sum of the transfer rates away from chromophore i. The two common transfer rates are Forster transfer given by

$$k(r) \propto R_0^6/R^6 \tag{13}$$

which is a long-range transfer and Dexter transfer given by

$$k(r) \propto e^{-\alpha r} \tag{14}$$

(normally attributed to triplet–triplet transfer) and is a short-range transfer.[11] For computational simplicity the transfer rate is set to one for chromophores that are one lattice site away and zero for all others. This could correspond to either the Dexter mechanism or Forster transfer with a small R_0. The traps have the same transfer rate as the other chromophores except that transfer is only into

Table I
Chromophore Contacts, Radius of Gyration, and Fluorescence Decay Moments as Functions of N and ϕ

N	ϕ	$\langle C_i \rangle$	$\langle R^2 \rangle$	$\langle M_0 \rangle$	$\langle M_1 \rangle$	$\langle M_2 \rangle$
50	$-\infty$	1.960	29.29	1.898×10^2	8.090×10^4	9.309×10^7
50	−0.5	2.126	22.43	1.538×10^2	5.501×10^4	5.327×10^7
50	0.0	2.308	18.24	1.156×10^2	3.287×10^4	2.685×10^7
50	0.275	2.570	13.48	75.26	1.527×10^4	9.705×10^6
50	0.35	2.667	11.97	64.77	1.135×10^4	6.254×10^6
50	0.5	2.952	8.613	40.03	4.767×10^3	2.195×10^6
100	$-\infty$	1.980	69.82	7.115×10^2	1.186×10^6	5.415×10^9
100	−0.5	2.156	56.94	5.385×10^2	6.855×10^5	2.473×10^9
100	0.0	2.354	41.92	4.118×10^2	4.245×10^5	1.267×10^9
100	0.275	2.662	28.05	2.507×10^2	1.807×10^5	4.060×10^8
100	0.35	2.842	22.46	1.804×10^2	9.768×10^4	1.707×10^8
100	0.5	3.284	12.98	73.85	1.808×10^4	1.970×10^7
200	$-\infty$	1.990	1.692×10^2	2.955×10^3	2.011×10^7	3.700×10^{11}
200	−0.5	2.166	1.252×10^2	2.307×10^3	1.254×10^7	1.806×10^{11}
200	0.0	2.374	94.54	1.690×10^3	7.096×10^6	8.265×10^{10}
200	0.275	2.727	57.27	8.057×10^2	1.842×10^6	1.286×10^{10}
200	0.35	2.949	40.47	4.815×10^2	7.778×10^5	4.257×10^9
200	0.5	3.616	16.09	1.016×10^2	2.779×10^4	4.485×10^7
400	$-\infty$	1.995	3.958×10^2	1.177×10^4	3.209×10^8	2.368×10^{13}
400	−0.5	2.199	2.997×10^2	7.011×10^3	1.175×10^8	5.898×10^{12}
400	0.0	2.392	2.079×10^2	5.938×10^3	8.617×10^7	3.501×10^{12}
400	0.275	2.767	1.173×10^2	2.504×10^3	1.876×10^7	4.414×10^{11}
400	0.35	3.102	63.56	1.012×10^3	3.811×10^6	5.488×10^{10}
400	0.5	3.763	30.85	2.440×10^2	1.429×10^5	3.704×10^8
error[a]		0.1–2%	1–10%	1–10%	2–20%	4–50%

[a] Error estimated from standard deviation of replica runs. The error increases with N; lower value corresponds to $N = 50$, upper value to $N = 400$.

the traps and never out. This results in a nonsymmetric transfer matrix. However, since the quantity of interest is the sum of the probabilities of an excitation residing on a normal chromophore, the traps are not included in the transfer matrix except in the diagonal elements of the chromophores they neighbor.

Obviously for our model of EET a critical characteristic of the coil is the number of non-nearest-neighbor contacts. In Figure 1 we have plotted the average number of contacts per chromophore ($\langle C_i \rangle$) as a function of ϕ for N from 50 to 400. $\langle C_i \rangle$ increases smoothly as one approaches the Θ-condition ($\phi = 0.275$). For all ϕ values $\langle C_i \rangle$ increases with N, presumably as a result of the larger number of opportunities for non-nearest-neighbor contacts. The dependence of $\langle C_i \rangle$ on N and ϕ is very important in the context of the present model because only non-nearest-neighbor contacts perturb the one-dimensional nature of the EET process.

Results

General Discussion of Data Analysis. The calculations described in the previous sections can be thought of most conveniently as a series of numerical experiments. For the particular polymer model presented in Methods, part B, we have determined accurate excitation survival probabilities over a large time regime for an extensive set of parameter values. The task to be addressed now is the utilization of these results in a manner that will facilitate analysis of experimental data for actual polymeric systems.

The most direct approach to modeling experimental decay curves with our methodology would be to carry out a large number of numerical simulations of the time-dependent fluorescence $S(t)$, convolute the results with the instrument response function, and compare the output with the experimental curve until agreement is obtained. While this is certainly feasible (and may be attempted for some cases), it has several defects as a general strategy. First, such a procedure would be relatively expensive computationally, particularly for large systems, and would not be accessible at all to workers lacking a version of our computer programs. Second, no physical insight into the factors controlling the decay curves and the relationship of these factors to the polymer geometry would be obtained. Finally, it would not be possible to fit transport in polymeric systems into a general framework of dynamical processes in disordered media.

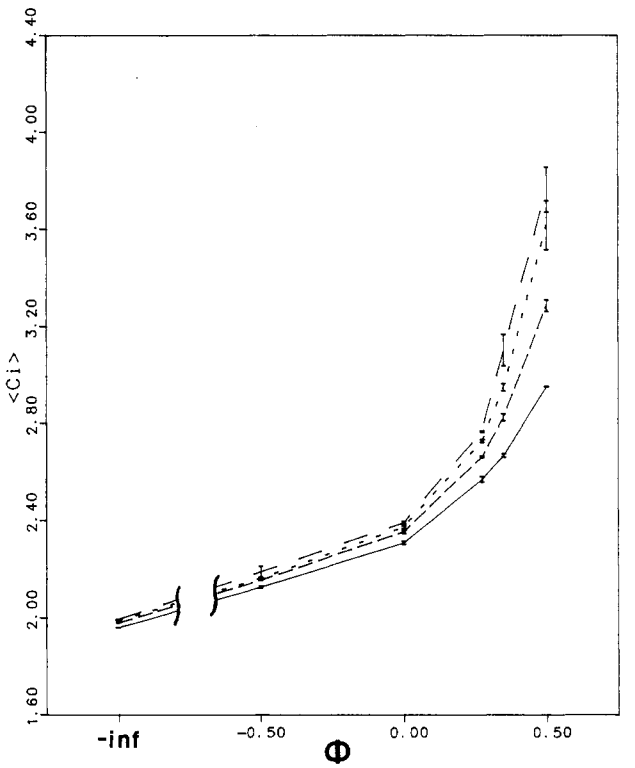

Figure 1. Average number of contacts per chromophore $\langle C_i \rangle$ as a function of ϕ, for $N = 400$, 200, 100, and 50 (from upper to lower) indicated. Note that the maximum and minimum values of $\langle C_i \rangle$ are approximately 3.6 and 2, respectively.

In this section, we examine a number of approaches to the analysis of our numerical data and the implications of this analysis for applications to experimental work. We show that a simplistic treatment of a finite polymer chain as a self-similar object is not in general adequate, although useful information can be obtained if this procedure is applied over a restricted time regime. On the other hand, a generalized concept of a time-dependent fractal dimension leads to a potentially very useful method of data analysis over the entire range of accessible data. The feasibility of utilizing this method to study realistic experimental results is investigated by a comparison with standard approaches to the analysis of fluorescence decay curves. The inadequacies of these latter type of fits are discussed and a new proposal for a practical fitting algorithm is made.

Discussion of Eigenvalues Distribution. The fundamental information that is obtained from the solution of eq 3 is the eigenvalue and the residue described by eq 7 such that the decay function $G_{ff}(t)$ is a sum over a large number of exponentially decaying functions. It has been quite common in polymer photophysics to describe fluorescence decay by a small number of exponentials (two or three). More recently Ware and co-workers[12] have used a distribution of exponentials to analyze fluorescence decay curves obtained by the single photon counting method for surface-bound species. Distributions of lifetimes have been used for years in the analysis of frequency-domain fluorescence spectroscopy.[13] Since there exist methods for direct extraction of the lifetime distribution, it is useful to discuss the general form of the distribution of $R_{ff}^{(j)}$ and λ_j. Typical plots of $R_{ff}^{(j)}$ versus λ_j are presented in Figure 2 for $N = 100$ and several representative ϕ values. As can be seen these distributions are sharply peaked at the lowest eigenvalue and decay rapidly for higher λ_j. As expected a larger ϕ value enhances the importance of the higher λ_j, which corresponds to a more rapidly decaying $G_{ff}(t)$ function. This is illustrated by the $G_{ff}(t)$ functions in Figure 3. An important feature of the above plots is the asymmetry in $R_{ff}^{(j)}$. Earlier work has usually assumed a symmetric distribution of lifetimes around a single most probable lifetime (described via a Gaussian or Lorentzian function), presumably as a result of different local environments. Our model also has dispersion in it, due to the configurational average over different coil geometries. However, this dispersion is convoluted with an underlying systematic envelope which reflects the mean polymer geometry and the trap concentration. The extraction of this aspect of the distribution from experimental data would obviously be of use in assessing the validity of differing physical models of a disordered (but not completely randomized) chromophore distribution. The results in Figure 2 suggest that experimentally derived lifetime distributions can in fact be directly used to characterize a polymer ensemble, if interpreted by a model in the manner described above. That is, a clear correlation between ϕ and the shape of the R_{ff} curves is present, and the change in line shape appears to be quantitatively significant enough to survive experimental noise. Alternatively, one might carry out a Laplace transform of the lifetime distribution to obtain an unbiased decay curve in the time domain deconvoluted from the instrument response function; an approach based along these lines is given below. Investigation of actual experimental data and a greater diversity of polymer models will be required before a definitive choice between these alternatives can be made.

Dependence of the Moments of the Decay Function on Coil Parameters. As was discussed in the preceeding section, the time dependence of the decay induced by the EET to traps is a complex, highly nonexponential function. While there are a variety of ways in which an experimental decay curve can be fit, one straightforward method of analysis is via the moments of $S(t)$, i.e.

$$M_n = \int_0^\infty t^n S(t)\, dt \tag{15}$$

where $S(0) = 1$. It turns out that for the model of EET discussed herein the moments behave in a very systematic way, which suggests that these quantities may be quite useful in characterizing polymer systems. One may anticipate that the higher moments may be difficult to extract experimentally because of poor signal-to-noise ratios at long times; thus, we will emphasize the behavior of M_0 and M_1 in this discussion. Note that M_0 and M_1/M_0 represent the quantum yield of fluorescence and the average lifetime of fluorescence decay in the limit that the intrinsic lifetime of the excited state (τ_0) is infinite. In order to utilize the relations to be discussed below the experimentalist would have to know the value of τ_0 (presumably obtained from a model system in which EET is absent) and know how τ_0 changes with the thermodynamic parameter ϕ (e.g., solvent, pH, etc.). Then the experimental decay curve should be multiplied by e^{t/τ_0} to obtain $S(t)$ and thence M_0, M_1, etc. While this is a demanding procedure, it is common to all theoretical interpretations of EET in real physical systems.[14]

The values of $M_0 - M_2$ are presented in Table I for randomly placed traps. The trends for end-placed traps are similar, although the decay is always slower for this case.[15] The values are in units of τ_S, the fundamental transfer time. As expected from the general behavior of $S(t)$, all moments decrease with increasing ϕ (more rapid trapping) and increase with chain length (larger average separation of initially excited chromophore and trap site). The lower moments (0–2) for end traps are always substantially larger than for randomly placed traps, while the situation reverses for the higher ones. This is the case because the end-trap case has a substantially longer tail in the decay curve compared to the random-trap case.

When one compares the trends in the "thermodynamic quantitites" like $\langle R^2 \rangle$ with ϕ to the moments there is an obvious similarity, i.e., as $\langle R^2 \rangle$ decreases both M_0 and M_1/M_0 decrease. This similarity is more striking when these values are scaled between the "extended chain limit" ($\phi \to -\infty$), and the collapsed chain ($\phi = +0.5$):

$$\langle R^2 \rangle = (\langle R^2 \rangle_\phi - \langle R^2 \rangle_{min})/(\langle R^2 \rangle_{max} - \langle R^2 \rangle_{min}) \tag{16}$$

with a similar definition for M_0, $\langle \tau \rangle$. For the latter $\langle \tau \rangle = M_1/M_0$. In Figure 4 these three quantities are plotted versus ϕ. As can be seen, there is almost no dependence on chain length in this presentation of the properties of the model. This suggests that the present model could be tested for a polydisperse polymer sample with nonuniform trap density if the density of traps is not a property of solvent quality. Unfortunately this is not the case for the most common trapping experiment in polymers, in which the trap is an excimer-forming site, the density of which is expected to increase as solvent quality decreases.

While it is quite clear that the time dependence of an excited state is predicted to be highly dependent on the coil density, it is less clear if one can detect the transformation from an almost purely one-dimensional system (very negative ϕ) to a disordered three-dimensional one (very positive ϕ). One method is to examine the distribution of eigenvalues and compare that distribution to the analytical solutions of Pearlstein et al.[16] Another is to fit $S(t)$ to an expression that contains the dimensionality

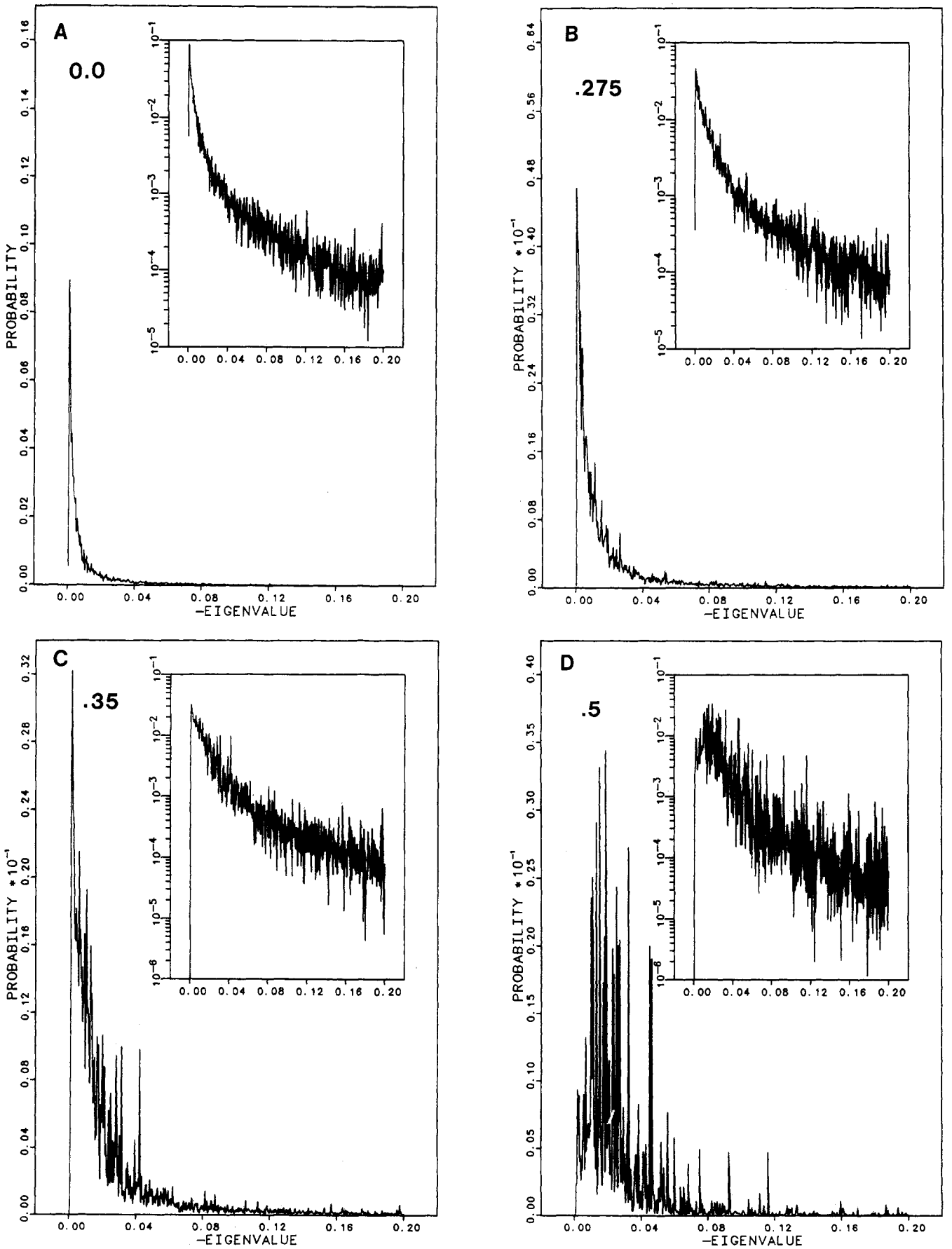

Figure 2. Plot of weighting factor $R_{ff}^{(j)}$ (probability) versus λ_j (eigenvalue) for $N = 100$ and ϕ value indicated. The eigenvalues are in units of w, the intrinsic nearest-neighbor transfer rate.

explicitly (see next subsection). In the context of the discussion of moments we note the following: for $\phi \leq 0$ the quantity M_1/M_0^2 is remarkably constant and seems to converge to ~2.3 for random traps and ~1.2 for end traps as $\phi \to -\infty$ regardless of chain length (see Figure 5 for the random-trap case). These results are consistent with the

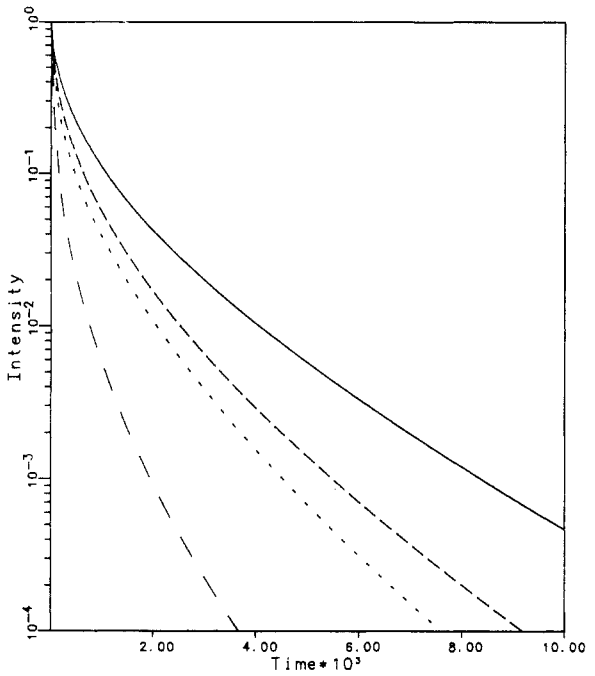

Figure 3. $G_{ff}(t)$ functions that correspond to parameter sets in Figure 2. For upper to lower curve, ϕ = 0, 0.275, 0.350, 0.500.

work of Pearlstein[16a] for impurity quenching on one-dimensional lattices in which it is shown that the nth moment is proportional to N^{2n+2}. Thus it follows that the M_1/M_0^2 ratio provides a test for the treatment of a polymer coil as a one-dimensional lattice.

Fractal Approach. There has recently been great interest in characterizing disordered materials via an effective nonintegral dimensionality. For structures which appear identical on all length scales (i.e., those which are self-similar), such a nonintegral dimension can be rigorously defined.[17-22] Transport properties are in general controlled by two nonintegral dimensions: the spectral dimension (which is related to the eigenvalue density of states of the linear operator describing the transport) and the Hausdorff or fractal dimension (which reflects the spatial organization of the corresponding eigenvectors). Diffusive behavior on truly self-similar lattices can be accurately described by simple power laws involving these two quantities. Examples of self-similar structures include the Sierpinski gasket[21] and a substitutionally disordered lattice with a fraction of occupied sites equal to the critical percolation density.[17-22]

When the structure in question deviates from self-similarity, modeling of transport behavior becomes much more complicated. For example, if one considers a substitutionally disordered lattice at a density of occupied sites that is greater than the percolation density, the diffusive behavior (e.g., mean-square displacement as a function of time) will exhibit a transition from an anomalous or fractional power law to a normal Euclidian one ($\langle R^2(t)\rangle \sim Dt$) as time increases.[17-22] One way of understanding this is to argue that the effective dimensionality is fractal on short length scales and becomes Euclidian on larger ones. Rather than considering one or two controlling nonintegral dimensions, in this context it seems more useful to think of the effective dimensionality as a continuously deformable function of time, reflecting a gradual transition to the ultimate Euclidian limit. This is in fact what is observed in accurate numerical simulations of finite time transport on disordered lattices.[23]

The position of onset and length of the transitional region depend upon how close one is to true self-similarity.

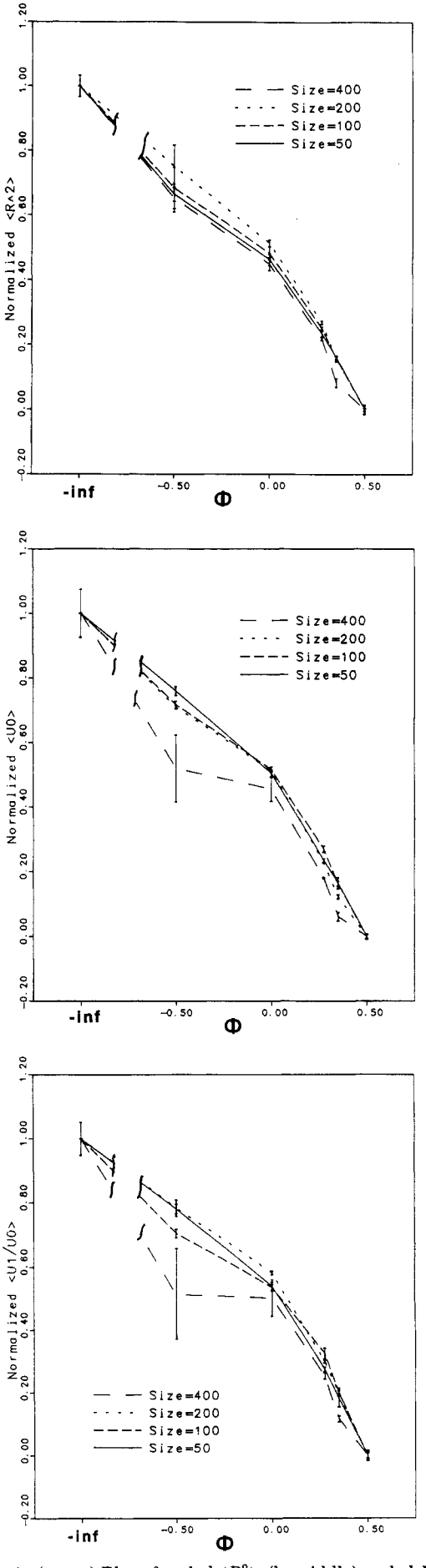

Figure 4. (a, top) Plot of scaled $\langle R^2\rangle$; (b, middle) scaled M_0; (c, bottom) scaled $\langle \tau \rangle$ versus ϕ.

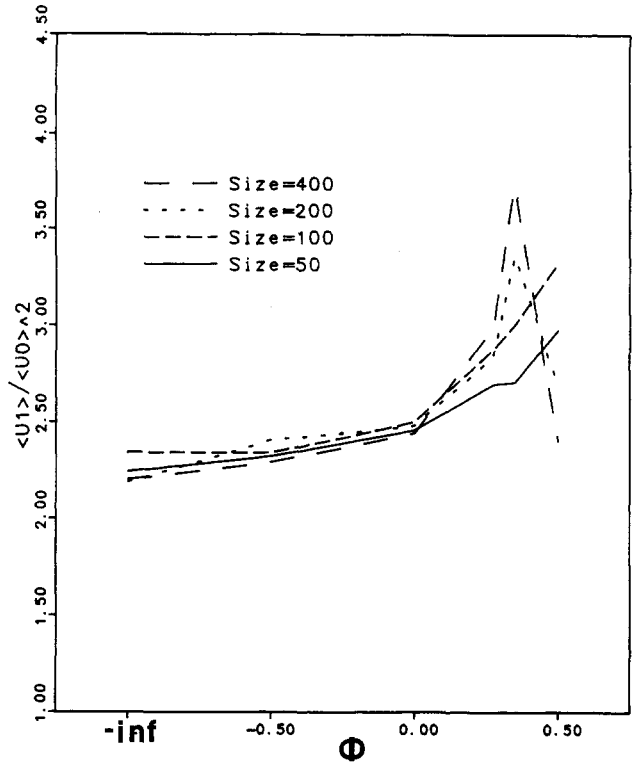

Figure 5. Plot of M_1/M_0^2 as a function of ϕ.

For the percolation problem, a difference of a few percent in density from the critical value leads to substantial deviations from pure self-similar behavior at relatively short times. The question of applicability to experimental systems depends upon factors like the time scale of the experiment and control over parameter accuracy. Our conclusion for the infinite percolative systems is that while it may be possible to observe purely self-similar transport under carefully controlled conditions, it is not the normal state of affairs; this means that a more complicated analysis must be utilized to interpret results quantitatively. The situation described below is even more difficult than the infinite lattice case because of the existence of finite size effects.

A. Self-Similar Analysis. To investigate the utility of a self-similar approach, we follow the cumulant expansion development of Klafter and co-workers[24] which they applied to trapping on a Sierpinski gasket. The survival probability is expressed as a functional of S_N, the number of distinct sites visited by the excitation after N steps. The first cumulant is proportional to the average of S_N over all walks, the second cumulant to the variance of S_N, and so on.

For a self-similar structure, $\langle S_N \rangle$ has been shown to depend on time via the power law[21]

$$\langle S_N \rangle \sim t^{d_s/2} \tag{17}$$

where d_s is the spectral dimension. The higher cumulants can similarly be shown to be proportional to this quantity raised to the appropriate power; e.g., the second cumulant scales as t^{d_s}. The appropriate function for the survival probability is then[24]

$$S(t) \sim \exp(-At^{d_s/2} + Bt^{d_s} - Ct^{3d_s/2} + ...) \tag{18}$$

where A, B, C, and d_s are to be treated as adjustable fitting parameters which are greater than zero.

It was in general possible to obtain very good fits of the simulated decay curves to an expression of this form. Initially we utilized a nonlinear least-squares fitting routine to determine the "best fit" parameters. Unfortunately, the values of d_s so obtained have a bizzare behavior as a function of ϕ. One would expect that d_s should monotonically increase as the nonbonded interactions are varied from negative (favoring a nearly one-dimensional chain) to positive (leading to some collapse of the coil). Instead, the obtained values actually go through a minimum near $\phi = 0.275$.

This behavior can be shown to be an artifact of the fitting procedure by examining the residual as a systematic function of an assumed d_s. The most striking conclusion from this study is the existence of a double minimum and the overall instability of the fitting procedure as reflected in the shallowness of the minima in the residual. The assumed functional form succeeds in reproducing the exact results by virtue of the large number of flexible fitting parameters and the restricted time regime to be fit. Our conclusion is that the d_s extracted from this procedure applied in the fashion described above has little physical meaning *for the systems considered in this paper* and that characterization of the polymer ensemble by a single spectral dimension is inappropriate. Note that there is no implication that similar difficulties exist for the work of Zumhofen et al.;[24,25] the Sierpinski gasket is a very different system.

Stable behavior of d_s results from reducing the size of the time interval over which the fitting procedure is attempted. This means that, e.g., fits utilizing only short time data can yield meaningful d_s values; it is argued below that application of the self-similar analysis to experiment has often been successful for just this reason. The question of how to choose the ideal time interval over which the fitting procedure should be carried out is nontrivial and depends upon experimental as well as theoretical considerations. We will return to this issue in the next section, after presenting an approach which is capable of locating the onset of finite-size effects and hence of addressing this problem directly.

B. Time-Dependent Fractal Dimensionality. A different approach to analyzing decay curves in a disordered system is to allow the exponent d_s in eq 18 to become time dependent. This procedure can be rationalized in a variety of physical and mathematical ways; some of these will be discussed in what follows. As a generalization of the viewpoint described above, the basic idea is that at different times the probability distribution propagated by the disordered master equation is altered, and thus the length scales which define the appropriate power law behavior of transport and trapping change continuously. If each length scale can be thought of as possessing an effective dimensionality, the use of a time-dependent exponent to model transport processes becomes natural. The approach has been used to describe the finite time behavior of transport observables on substitutionally disordered lattices by several workers.[20,23,26]

We first present the details of the numerical algorithm used to process the data for the trapping problem. The assumed functional form of the survival probability is

$$S(t) \sim \exp(A(t)t^{\alpha(t)}) \tag{19}$$

where A and α are parametric functions to be determined. The logarithm of ln S is plotted versus the logarithm of t, and least-squares fits to a linear functional form are carried out for a series of time windows. The size of the time windows is important in producing useful results; it should be small enough so as not to extend over substantial variations of the effective exponent α but large enough to smooth out noise and/or uninteresting transient effects. The invariance of A and α to the choice of a reasonable

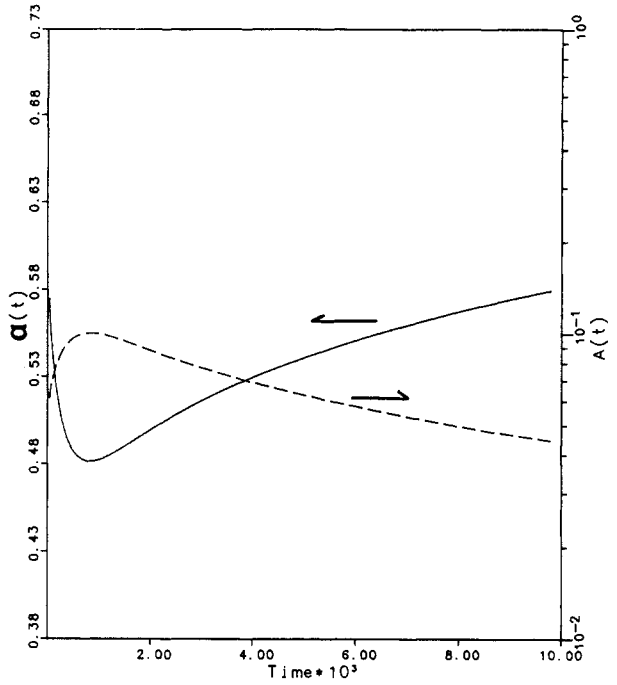

Figure 6. Plot of $\alpha(t)$, $A(t)$ for $N = 100$, $\phi = 0.275$.

range of time window was taken as the criterion for stability of these fitting parameters.

The form of eq 19 is very general and the interpretation of the parameters depends on the context of the problem since this function clearly can fit any nonexponential decay, no matter what the source of the nonexponentiality is (e.g., EET, inhomogeneous broadening, excimer dissociation processes, etc.). In the following we will emphasize the interpretation of $\alpha(t)$ in terms of an effective spectral dimension, which we believe is appropriate for the model we are considering.

In simple cases, $A(t)$ will be a constant or a slowly varying function which is more strongly dependent upon the trap density and the hopping rate. This is not the case for the present system; finite size effects and the variation of the effective dimensionality lead to significant variation in A over moderate time intervals. $A(t)$ typically mirrors the behavior of $\alpha(t)$ in a trivial fashion, essentially as the intercept of a tangent line to a curve will systematically track the slope of the tangent line (which is derived from the curve) (for an example see Figure 6). Our present view is therefore that the time dependence of A contains no additional information beyond that present in α.

A rigorous theoretical justification of the interpretations of the $\alpha(t)$ function which we present here it not now available. Thus, the utility of the approach will be demonstrated in a phenomenological fashion, i.e., by displaying the regular behavior of the function as the polymer size and geometry is varied. Hopefully, these results will stimulate analytic theoreticians to investigate the underlying mathematics of the procedure in the future.

An examination of our data reveals significant regularities in the form of $\alpha(t)$ and its behavior as a function of polymer size and geometry. The features uncovered by this reprocessing of the data are not easily accessible from either the original decay curves or from the self-similar fractal analysis (e.g., eq 18). We shall proceed by first characterizing these features more quantitatively, followed by a physical interpretation and a mathematical analysis.

Most of the $\alpha(t)$ curves display an initial decay from a value between 0.5 and 1.0 followed by a rise to unity after passing through a single minimum.[27] In a few cases there is a very short initial rise before this pattern is displayed.

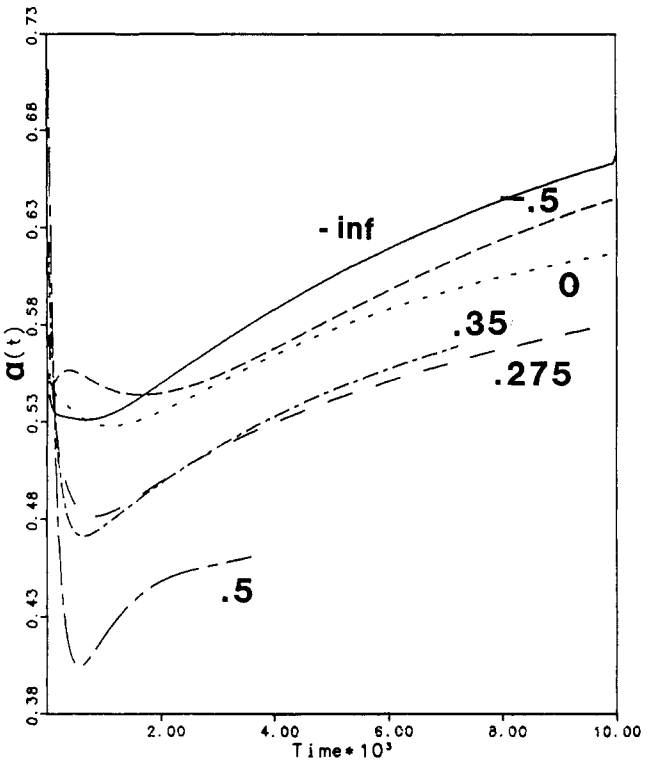

Figure 7. $\alpha(t)$ for $N = 100$, ϕ value indicated, and random placement of traps. The maximum time for the truncated plot is such that $S(t) = 10^{-4}$.

This rise can be attributed to logarithmic corrections to the short-time mean-field behavior. We defer further discussion of this feature (which is a small effect quantitatively) to future studies. Typical $\alpha(t)$ curves for $N = 100$ are displayed in Figure 7.

Given the above observations, it is reasonable to characterize the $\alpha(t)$ curves by the following parameter set: (1) value of α at $t = 0$ (α_i); (2) value of α at the minimum (α_m); (3) value of the time at the minimum (t_m). Figure 8 displays plots of the three characteristic parameters as a function of ϕ for each value of N that we have studied.

The generic functional behavior of $\alpha(t)$ is readily understood. The initial value of α reflects short time behavior averaged over a small window; the relevance of the window size will be discussed below. For sufficiently short time, the first cumulant approximation described above (equivalent to the mean field or Rosenstock approximation[28]) should be valid. We therefore suggest that the *initial* value of α (designated α_i) be interpreted as analogous to the quantity $d_s/2$ presented in an earlier section. Another way of looking at this is that analysis of data from sufficiently short time can yield a stable estimate of the analogue of the spectral dimension for systems which deviate from self-similarity. We shall have more to say concerning this point when we discuss the processing of experimental data.

The numerical results of Figure 8 for α_i are in accord with these statements. First, α_i as a function of ϕ rises monotonically from a value near 0.5 to one somewhat less than unity for all polymer lengths, thus increasing from the purely one-dimensional value of 0.5 to the value of 1.0 expected for a three-dimensional system with random traps.[26] For $\phi < 0.0$, α_i displays a small decrease as a function of chain length. This can be understood as a convergence to the true one-dimensional value for an infinite system; finite size effects and residual cross-chain transfers will tend to increase α_i by mixing in some exponential character (for which $\alpha = 1$). For large positive

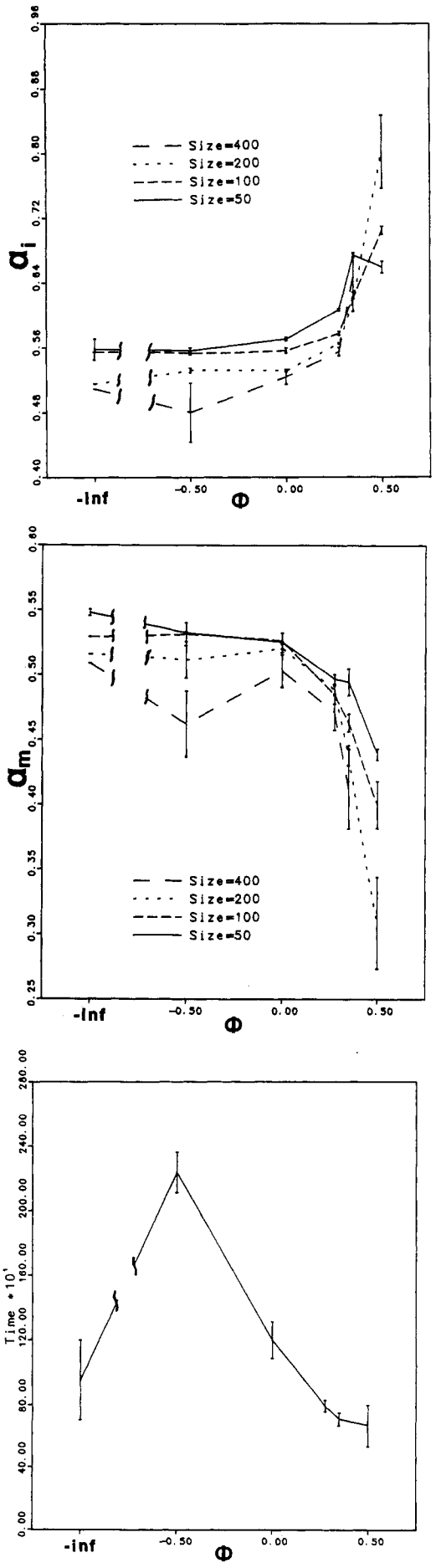

Figure 8. Plot of α_i, α_m, and t_m as a function of ϕ for N values indicated. For t_m only $N = 100$.

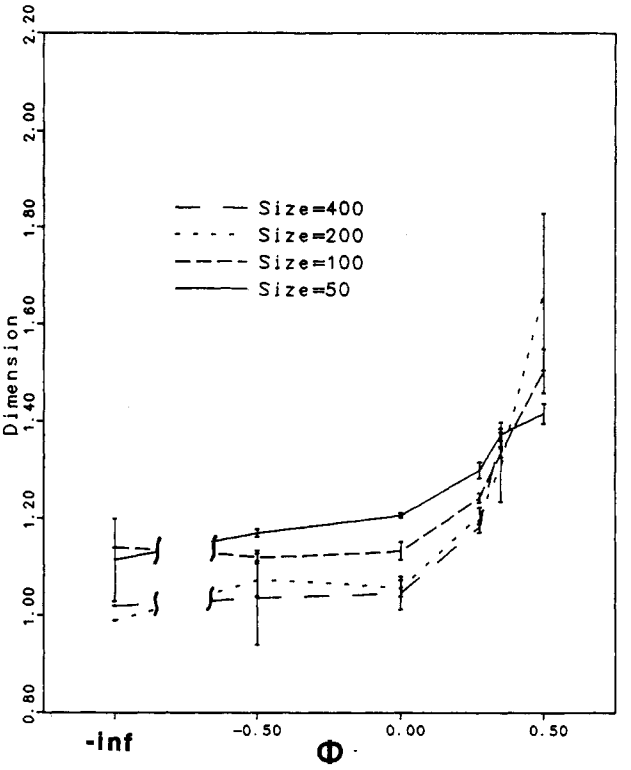

Figure 9. Plot of effective dimension (d_s) versus ϕ for indicated N values.

ϕ, on the other hand, the reverse trend holds, i.e., α_i increases substantially with increasing N. The dominant effect in this case is an actual increase in effective dimensionality as N increases, due essentially to a reduced surface-to-volume ratio. This is quantitatively reflected in the data in Table I (or Figure 1) which displays the average number of contacts per monomer as a function of polymer size. The effect is most striking for $\phi = +0.5$, as is the corresponding increase in α_i.

The subsequent decay of $\alpha(t)$ to a minimum can be examined from several different perspectives. From the standpoint of a cumulant expansion, this behavior reflects the growing importance of the second cumulant which has a sign opposite to the first. Mathematically, one has a quadratic form which is moving toward its minimum value as t increases. The difficulties encountered in using the self-similar expression for the cumulant (eq 18) show that the particular functional form invoked is not entirely adequate; however, the basic conceptual picture is still useful. As can be seen from Figure 8, the behavior of α_m is quite regular.

The final rise in α is attributable to finite size effects. As t goes to infinity, α must approach unity for a finite system, reflecting the dominance of a single (smallest) eigenvalue. The point at which this occurs depends upon the system size and the effective dimensionality; for a collapsed polymer the smallest eigenvalue will have a larger magnitude than for an extended value (this is easily seen by considering ordered three- and one-dimensional systems with the same number of sites). Both trends are reflected in Figure 8, which plots the time t_m at which the minimum occurs versus ϕ for various values of N.

To further investigate the usefulness of a single spectral dimension to characterize the data sets generated in this paper, we have carried out nonlinear least-squares fits to eq 18, but using only the time interval from 0 to t_{min}.

The results of these calculations are displayed in Table II and Figure 9, which plots the effective dimension versus ϕ for various values of N. A striking regularity in d_s is now

Table II
Values of Fitting Parameters of Equation 18 as Function of N and ϕ (See Text)

N	ϕ	d_s	A	B	C
50	$-\infty$	1.115	6.897×10^{-2}	-4.931×10^{-4}	-1.321×10^{-5}
50	-0.5	1.170	7.739×10^{-2}	3.948×10^{-4}	2.785×10^{-6}
50	0.0	1.207	8.722×10^{-2}	6.233×10^{-4}	4.941×10^{-6}
50	0.275	1.300	9.987×10^{-2}	1.048×10^{-3}	8.004×10^{-6}
50	0.35	1.373	9.968×10^{-2}	1.266×10^{-3}	1.037×10^{-5}
50	0.5	1.417	1.198×10^{-1}	1.292×10^{-3}	7.368×10^{-6}
100	$-\infty$	1.120	3.526×10^{-2}	6.225×10^{-5}	2.492×10^{-7}
100	-0.5	1.120	3.949×10^{-2}	4.000×10^{-7}	-2.258×10^{-7}
100	0.0	1.133	4.770×10^{-2}	9.362×10^{-5}	3.118×10^{-7}
100	0.275	1.243	5.561×10^{-2}	3.611×10^{-4}	1.798×10^{-6}
100	0.35	1.337	5.603×10^{-2}	3.898×10^{-4}	1.644×10^{-6}
100	0.5	1.503	6.659×10^{-2}	4.202×10^{-4}	1.237×10^{-6}
200	$-\infty$	1.050	1.931×10^{-2}	-2.391×10^{-5}	-2.569×10^{-8}
200	-0.5	1.073	2.046×10^{-2}	-3.079×10^{-5}	-1.916×10^{-7}
200	0.0	1.057	2.645×10^{-2}	-1.682×10^{-5}	-1.250×10^{-7}
200	0.275	1.207	3.027×10^{-2}	1.089×10^{-4}	3.372×10^{-7}
200	0.35	1.307	3.290×10^{-2}	1.232×10^{-4}	2.783×10^{-7}
200	0.5	1.667	3.421×10^{-2}	8.479×10^{-5}	9.096×10^{-8}
400	$-\infty$	1.050	9.571×10^{-3}	7.245×10^{-7}	2.130×10^{-8}
400	-0.5	1.037	1.284×10^{-2}	4.911×10^{-5}	5.649×10^{-7}
400	0.0	1.047	1.357×10^{-2}	-4.671×10^{-6}	-3.871×10^{-8}
400	0.275	1.183	1.734×10^{-2}	4.015×10^{-5}	7.736×10^{-8}
400	0.35	1.373	1.628×10^{-2}	3.015×10^{-5}	2.905×10^{-8}

obtained; in fact, the results are almost identical with those for α_i, as would be expected from the previous discussion. In effect, one is using a rather large "window" to capture the short to intermediate time effective dimensionality. A similar observation has been made in the investigation of the effective dimensionality for trapping on two-dimensional percolating lattices.[29,30] We defer a quantitative comparison of the value of the d_s obtained via this procedure as compared to α_i to another paper. For now, we conclude that the use of a cumulant-type stretched-exponential expression is reasonable provided that the time interval over which the fitting is done is sufficiently small.

A Proposed Methodology for Experimental Data Analysis

We turn now to the practical question of analysis of experimental data. We first consider the validity of existing procedures in light of the above results; this is followed by a suggested alternate approach.

We have shown that the use of a single fractal dimension to fit over a long time period is not a stable procedure. However, a fit over a short time domain (e.g., before the minimum in $\alpha(t)$ is approached) is a feasible way of obtaining a quantity similar to the initial exponent α_i which may be systematically correlated with the polymer geometry in a straightforward way. For example, the fractal analysis of Kamioka et al.[31] yields reasonable results for d_s as a function of solvent. An investigation of the actual time scale over which their fit is made (removing the influence of the monomer fluorescence lifetime) reveals that the entire region falls well with the criteria described above.

Another approach that has been frequently utilized is two- or three-exponential fits. For systems with a truly continuous distribution of trapping rates, this sort of analysis is unlikely to yield physical insight. On the other hand, the fact that such a functional form achieves a reasonably small residual is not surprising; as shown below, the function is compatible with our simulations except at short time.

Figure 10 displays a typical three-exponential fitting function (from Kamioka et al.[31]) analyzed to yield an $\alpha(t)$ function. The overall form of the curve is in good agreement with the theoretical simulations above. At short

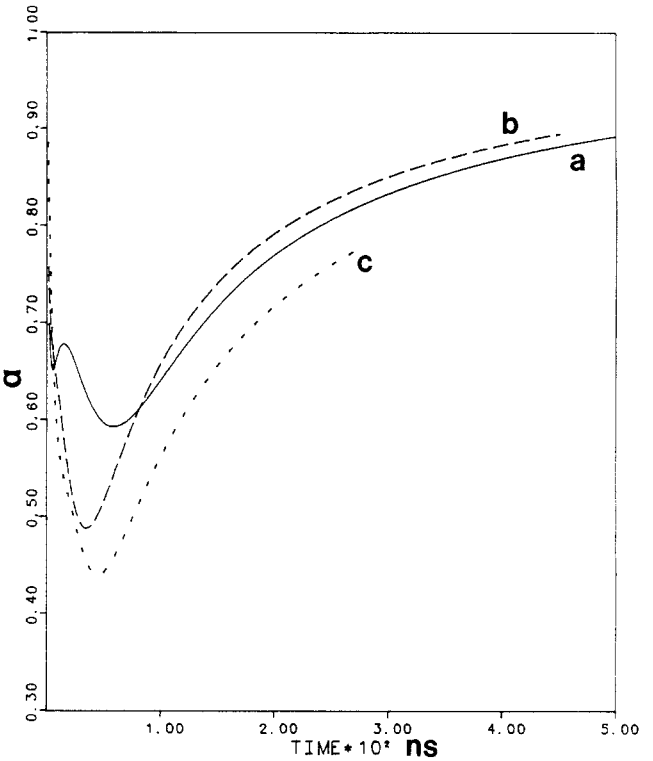

Figure 10. Analysis of three-exponential decay of Kamioka et al.[31] as the quantity $\alpha(t)$ (see text). The different solvents are (a) DMF (good solvent), (b) DMF/methanol (intermediate), and (c) methanol (poor solvent).

times the multiexponential function generates an $\alpha(t)$ of unity.[27] This is the result of the lack of a dense manifold of components with large exponents in the fitting function; a three-exponential fit is precluded by the assumed functional form from achieving a good fit at short times. It should be possible, however, to derive α_m and t_m from a multiexponential fit by the procedure used here. These quantities could then be correlated with the polymer conformation and size.

The above discussion indicates that specific fitting functions for analysis of experimental data may not be capable to extracting all of the useful information available in the decay curves. We propose instead that the raw data should be numerically deconvoluted from the instrument response function by an unbiased algorithm.[32] The resulting decay curve could then be processed into an $S(t)$ with the monomer lifetime component removed. Conversion of this data into an $\alpha(t)$ form would then permit direct application of the correlations shown above. For example, one could use the three characteristic parameters (α_i, α_m, t_m) to estimate a value of ϕ and N (if not known from other measurements) and then carry out direct simulations to refine the results.

This procedure is perhaps not needed if the polymer model is well understood and one wants to obtain limited properties (e.g., radius of gyration); the short time information suffices for such a situation. That is, one can probably use just α_i (or d_s obtained as described in this section) to infer ϕ, particularly if N is known. This is already implicit in the analysis of Kamioka et al.[31] cited above and in the analysis of the fluorescence short-time depolarization experiments of Fayer and co-workers[33] in which a cumulant expansion procedure is used to relate the decay of polarization to the polymer geometry.

However, there are many interesting cases for which a well-developed polymer model does not exist, e.g., polymer melts, polymer films on surfaces, formation of excimer

traps, polydisperse solutions, etc. It may be necessary in such cases to explore several qualitatively different models as well as refining parameter values for a given model. For these situations, our approach provides a practical method of distinguishing alternative polymer models. A correct model must be able to reproduce the entire $\alpha(t)$ curve (particualrly the key features identified above) as opposed to one segment of it. The systematic variation of parameters under experimental control (e.g., trap concentration) can provide cross checks on the validity of the model.

Our objective is the development of a comprehensive and reliable methodology for determination of polymer morphology from a set of experimental fluorescence decay curves. The suitability of the above approach must, of course, be tested by analyzing actual data, checking the conclusion with independent experiments if possible. This effort is currently in progress.

Acknowledgment. This research was supported by the National Science Foundation Division of Materials Research, Materials Research Group Program (DMR-8418086). S.E.W. also would like to acknowledge the support of the NSF Polymers Program (DMR-8614252). We thank the University of Texas Center for High Performance Computing for generously providing Cray-XMP supercomputer time.

References and Notes

(1) (a) Fitzgibbon, P. D.; Frank, C. W. *Macromolecules* **1982**, *15*, 733. (b) Gelles, R.; Frank, C. W. *Macromolecules* **1982**, *15*, 741. (c) Fredrickson, G. H.; Frank, C. W. *Macromolecules* **1983**, *16*, 572. (d) For a general review see: Frank, C. W.; Fredrickson, G. H.; Andersen, H. C. *Photophysical and Photochemical Tools in Polymer Science*; NATO ASI Series C.; Winnik, M. A., Ed.; D. Reidel: Dordrecht, Holland, 1986; Vol. 182.
(2) Rosenbluth, M. N.; Rosenbluth, A. W. *J. Chem. Phys.* **1968**, *49*, 648.
(3) McCrackin, F. L.; Mazur, J.; Guttman, C. M. *Macromolecules* **1973**, *6*, 859.
(4) An expanded discussion of these results will appear in: *Molecular Dynamics in Restricted Geometries*; Klafter, J., Drake, J. M., Eds.; Wiley: New York, in press.
(5) Paige, C. C. *Linear Algebra Appl.* **1980**, *34*, 235.
(6) Barth, W.; Martin, R. S.; Wilkinson, J. H. *Numer. Math.* **1967**, *9*, 386.
(7) Cullum, J.; Willoughby, R. A. *J. Comput. Phys.* **1981**, *44*, 329.
(8) Nauts, A. *Chem. Phys. Lett.* **1985**, *119*, 529.
(9) Nauts, A.; Chapuisat, X. *Phys. Rev. A* **1985**, *A32*, 3403.
(10) Nauts, A.; Wyatt, R. E. *Phys. Rev. Lett.* **1983**, *51*, 2238.
(11) (a) See Birks, J. B. *Photophysics of Aromatic Molecules*; Wiley-Interscience: New York, 1970. (b) Forster, T. *Ann. Phys. (Leipzig)* **1948**, *2*, 55. (c) Dexter, D. L. *J. Chem. Phys.* **1953**, *21*, 836.
(12) (a) James, D. R.; Ware, W. R. *Chem. Phys. Lett.* **1985**, *120*, 455. (b) James, D. R.; Liu, Y.-S.; DeMayo, P.; Ware, W. R. *Ibid.* **1985**, *120*, 460.
(13) See for example: Lakowicz, J. R.; Johnson, M. L.; Wiezk, W.; Bhat, A.; Steiner, R. F. *Chem. Phys. Lett.* **1987**, *138*, 587.
(14) Alternatively the experimental moments may be regarded as the e^{-t/τ_0} Laplace transform of the moments calculated herein.
(15) This is easily understood because the average separation of a randomly placed excitation to the trap is larger.
(16) (a) Pearlstein, R. M. *J. Chem. Phys.* **1972**, *56*, 2431. (b) Lakatos-Lindenberg, K.; Hemenger, R. P.; Pearlstein, R. M. *J. Chem. Phys.* **1972**, *56*, 4852.
(17) Havlin, S.; Ben-Avraham, D.; Sompolinsky, H. *Phys. Rev. A* **1983**, *27*, 1730.
(18) Gefen, Y.; Aharony, A.; Alexander, S. *Phys. Rev. Lett.* **1983**, *50*, 77.
(19) Alexander, S.; Orbach, R. *J. Phys. (Les Ulis, Fr.)* **1982**, *43*, L-625.
(20) Pandey, R. B., et al. *J. Stat. Phys.* **1984**, *34*, 427.
(21) Rammal, R.; Toulouse, G. *J. Phys. (Les Ulis, Fr.)* **1983**, *44*, L-13.
(22) Stanley, H. E. In *On Growth and Form*; Stanley, H. E., Ostrowsky, N., Eds.; Nyoff: Dordrecht, The Netherlands, 1986.
(23) Friedrichs, M. S.; Friesner, R. A. *Phys. Rev. B* **1988**, *37*, 308.
(24) Zumhofen, G.; Blumen, A.; Klafter, J. *J. Phys. A.: Math Gen.* **1984**, *178* L-479.
(25) Klafter, J.; Blumen, A.; Zumhofen, G. *J. Stat. Phys.* **1984**, *36*, 561.
(26) Argyrakis, P.; Kopelman, R. *J. Chem. Phys.* **1985**, *83*, 3099.
(27) It is easily shown that for times such that $t\lambda_{max} \ll 1$ (λ_{max} is the largest eigenvalue) $\alpha = 0$ and $A = M_0$. This limit is important for decay functions containing a small number of exponentials (such as typically used to describe experimental data) but not for decay functions generated from a large transfer rate matrix such as used here.
(28) Rosenstock, H. B. *Phys. Rev.* **1969**, *187*, 1166.
(29) Friedrichs, M. S.; Friesner, R. A. *Chem. Phys. Lett.* **1987**, *137*, 285.
(30) Friedrichs, M. S.; Friesner, R. A. *Chem. Phys.* in press.
(31) Kamioka, K.; Webber, S. E.; Morishima, Y. *Macromolecules* **1988**, *21*, 972.
(32) A direct numerical deconvolution could be used. Alternately a distribution function of lifetimes[12,13] can be used or the decay curve could be fit piecewise for a range of time windows.
(33) (a) Peterson, K. A.; Zimmt, M. B.; Linse, S.; Domingue, R. P.; Fayer, M. D. *Macromolecules* **1987**, *20*, 168. (b) Peterson, K. A.; Fayer, M. D. In *Photophysics of Polymer Systems*; ACS Monograph Series 358; American Chemical Society: Washington, DC, 1987.